

- <sup>4</sup>S. Adya, Phys. Rev. 166, 991 (1968).  
<sup>5</sup>V. A. Allesandrini, C. A. Garcia, and H. Fanchiotti, Phys. Rev. 170, 935 (1968).  
<sup>6</sup>K. A. A. Hamza and S. Edwards, Phys. Rev. 181, 1494 (1969).  
<sup>7</sup>Z. Kopal, *Numerical Analysis* (John Wiley & Sons, Inc., New York, 1955).  
<sup>8</sup>D. Y. Wang, in *Three Particle Scattering in Quantum Mechanics*, edited by J. Gillespie and J. Nuttall (W. A. Benjamin, Inc., New York, 1968).  
<sup>9</sup>C. C. H. Leung and S. C. Park, Phys. Rev. 187, 1239 (1969).  
<sup>10</sup>D. P. Harrington, Phys. Rev. 147, 685 (1966).  
<sup>11</sup>C. Lovelace, Phys. Rev. 135, B1225 (1964).

PHYSICAL REVIEW C

VOLUME 4, NUMBER 2

AUGUST 1971

Exchange Processes in  $n + \alpha$  Scattering\*†

D. R. Thompson and Y. C. Tang

*School of Physics, University of Minnesota, Minneapolis, Minnesota 55455*

(Received 16 April 1971)

The features of the kernel function in the nonlocal  $n + \alpha$  interaction, derived with the resonating-group method, which uses a totally antisymmetric wave function and a nucleon-nucleon potential, is studied. This kernel function is made up of three terms, corresponding to knock-out, heavy-particle-pickup, and nucleon-rearrangement processes. In the medium- and high-energy regions, the knockout process contributes mainly in the forward directions, while the heavy-particle-pickup and nucleon-rearrangement processes contribute mainly in the backward directions. In particular, it is found that these latter two processes are almost entirely responsible for the occurrence of large backward-angle cross sections in the  $n + \alpha$  problem. An equivalent local potential between the neutron and the  $\alpha$  particle is also constructed, which, in the Born approximation, yields the same results as does the resonating-group calculation. This equivalent local potential has an explicit energy dependence and a significant amount of Majorana space-exchange component. Finally, approximation methods are proposed which contain the essential features of the antisymmetrization procedure and yet could be used to consider such more complicated problems as the scattering of nucleons by medium- and heavy-weight nuclei.

## I. INTRODUCTION

In recent years, a number of calculations<sup>1,2</sup> have been performed to examine the properties of light nuclear systems with  $A \leq 8$  using the method of the resonating-group structure.<sup>3,4</sup> The results of these calculations have been very encouraging, since for all these systems, the agreement between the calculated and experimental results was found to be quite satisfactory over a wide range of energies.

A logical step is to extend these calculations to heavier systems, such as the scattering of protons by medium- and heavy-weight nuclei where extensive phenomenological analyses have been performed using the optical model with local potentials.<sup>5</sup> Here, however, one encounters practical difficulties, since in a resonating-group calculation one employs a completely antisymmetric wave function which, from a computational point of view, is feasible only for systems with a relatively small number of nucleons. On the other hand, the results of the resonating-group calculations clearly indicated that the effects introduced by the antisymmetrization procedure are important and can-

not be omitted if satisfactory agreement with the experimental data is to be obtained. Thus, in a heavier system where there is no *a priori* reason to expect that the antisymmetrization effects are unimportant, one must seek an approximation method which can simplify the computation to a significant extent and yet preserve the main features of antisymmetrization. In this investigation, we make an initial attempt in this direction by performing a detailed study of the antisymmetrization effects in the case of the scattering of neutrons by  $\alpha$  particles. This particular case is chosen, since here these effects are manifested in a particularly transparent manner and hence are amenable to clear and simple interpretation.

In the one-channel resonating-group formalism, this complicated five-nucleon problem is reduced to a two-body problem in which the wave function  $F(\vec{R})$  describing the relative motion of the neutron and the  $\alpha$  particle is given by

$$\left[ \frac{\hbar^2}{2\mu} \nabla_R^2 + E - V_D(\vec{R}) \right] F(\vec{R}) = \int K(\vec{R}, \vec{R}') F(\vec{R}') d\vec{R}', \quad (1)$$

where  $\mu$  denotes the reduced mass and  $E$  denotes the relative energy of the two clusters in the c.m. system.<sup>6</sup> The meaning of this equation is that the neutron and the  $\alpha$  particle can be considered as structureless, provided that the interaction between them is represented by the direct potential  $V_D(\vec{R})$  together with a nonlocal potential characterized by the kernel  $K(\vec{R}, \vec{R}')$ . In Sec. II, we shall outline the derivation of these potential terms, with particular emphasis being paid to the structure of the kernel function. As will be shown there, this kernel function can in fact be separated into three parts, corresponding to knockout, heavy-particle-pickup, and nucleon-rearrangement processes.

For a semiquantitative understanding of the general features of this scattering problem, we have derived in Sec. III the scattering amplitudes for the direct and exchange processes in the energy range from 50 to 100 MeV with the first Born approximation.<sup>7</sup> From this study, we find that at these relatively high energies, the knockout process contributes mostly in the forward directions, while the heavy-particle-pickup process contributes mostly in the backward directions. Using the Born amplitudes, we have further constructed an equivalent local interaction between the neutron and the  $\alpha$  particle. This equivalent interaction has an expected energy dependence and contains a significant amount of Majorana space-exchange component.

The contribution to the differential cross section from the various exchange processes is further studied by a calculation in which Eq. (1) is solved numerically, but with the terms in the kernel function corresponding to these exchange processes successively set as zero. This is discussed in Sec. IV. From this calculation, we conclude that in the energy region of concern to us, the Born-approximation results are fairly reliable and, therefore, our findings about the characteristics of the various scattering amplitudes and the equivalent interaction between the clusters can be used as a guide to devise approximation methods for calculations in heavier systems.

In Sec. V we discuss two approximation methods which could be used to study the problems of the scattering of nucleons by medium- and heavy-weight nuclei and yet contain the essential features of the antisymmetrization procedure. One of these methods is tested on the  $n + \alpha$  scattering problem itself in the energy region of 20 to 100 MeV, and the results do agree very well with those obtained using the more complicated resonating-group approach.

Finally, in Sec. VI, we summarize and discuss the results of this investigation.

## II. FORMULATION

The formulation of the  $n + \alpha$  scattering problem in the one-channel approximation has been briefly described in our previous publication.<sup>6</sup> Here we shall fill in a few essential steps in order that the effects of antisymmetrization can become more transparent.

The wave function for the  $n + \alpha$  system is written as

$$\Psi = \alpha \{ \phi(1234) F(\vec{R}_\alpha - \vec{r}_5) \xi(s, t) \}, \quad (2)$$

where  $\alpha$  is an antisymmetrization operator and  $\xi$  is an appropriate charge-spin function which has the form

$$\begin{aligned} \xi(s, t) = & [ \delta(s_1, \frac{1}{2}) \delta(t_1, -\frac{1}{2}) \delta(s_2, \frac{1}{2}) \delta(t_2, \frac{1}{2}) \\ & \times \delta(s_3, -\frac{1}{2}) \delta(t_3, -\frac{1}{2}) \delta(s_4, -\frac{1}{2}) \delta(t_4, \frac{1}{2}) ] \\ & \times \delta(s_5, \frac{1}{2}) \delta(t_5, -\frac{1}{2}), \end{aligned} \quad (3)$$

with  $\delta(s, m_s)$  and  $\delta(t, m_t)$  denoting the spin and isospin functions, respectively. The function  $\phi(1234)$  describes the spatial behavior of the  $\alpha$  cluster and is chosen as

$$\phi(1234) = N^{-1} \exp[-\frac{1}{2} \alpha \sum_{i=1}^4 (\vec{r}_i - \vec{R}_\alpha)^2], \quad (4)$$

where  $\vec{R}_\alpha$  is the position vector of the center of mass of the  $\alpha$  cluster, and  $N$  is a normalization constant given by

$$N = (\pi^3/4\alpha^3)^{3/4}. \quad (5)$$

The width parameter  $\alpha$  is chosen to yield the experimentally determined value of the rms radius of the nucleon distribution in the  $\alpha$  particle; it is equal to  $0.514 \text{ F}^{-2}$ , which corresponds to a rms radius of  $1.48 \text{ F}$ .

The scattering function  $F(\vec{R}_\alpha - \vec{r}_5)$  in Eq. (2) is determined from the variational equation

$$\langle \delta\Psi | H - E' | \Psi \rangle = 0, \quad (6)$$

where  $E'$  is the total energy composed of the internal energy  $E_\alpha$  of the  $\alpha$  cluster and the relative energy  $E$  in the c.m. system, and  $H$  is the Hamiltonian given by

$$H = -\frac{\hbar^2}{2M} \sum_{i=1}^5 \nabla_i^2 + \sum_{i>j=1}^5 V_{ij}. \quad (7)$$

The nucleon-nucleon potential used here is chosen as

$$\begin{aligned} V_{ij} = & -V_0 e^{-\kappa r_{ij}^2} (w - m P_{ij}^s P_{ij}^t + b P_{ij}^s - h P_{ij}^t) \\ & + \frac{e^2}{4r_{ij}} (1 + \tau_{iz})(1 + \tau_{jz}), \end{aligned} \quad (8)$$

with  $V_0 = 72.98 \text{ MeV}$ ,  $\kappa = 0.46 \text{ F}^{-2}$ , and the constants

$w$ ,  $m$ ,  $b$ , and  $h$  satisfying the equations

$$\begin{aligned} w + m + b + h &= 1, \\ w + m - b - h &= 0.63. \end{aligned} \quad (9)$$

$P_{ij}^o$  and  $P_{ij}^r$  are the usual spin and isospin exchange operators, respectively. This potential was used in a number of our older calculations with the resonating-group method. In our more recent calculations,<sup>2,8</sup> we have instead employed a somewhat more complicated two-nucleon potential which fits the nucleon-nucleon scattering data better and which does yield improved results for the various scattering systems considered. In this investigation, however, since our main concern is to achieve an understanding of the features of the antisymmetrization effects rather than to obtain precise agreement with experiment, we shall simplify the problem as much as possible. Therefore, we choose to use the simpler potential of Eq. (8). Also, the exchange mixture will be fixed to be of the Serber type; small adjustment of this mixture to obtain the best agreement with experiment as was done in our previous calculations will not be carried out here.

For the spatial integration required in Eq. (6), it is convenient to use the three independent  $\alpha$ -particle internal coordinates  $\vec{r}_i$ , the relative coordinate  $\vec{R}$  and the c.m. coordinate  $\vec{R}_{c.m.}$ , defined as

$$\begin{aligned} \vec{r}_i &= \vec{r}_i - \vec{R}_\alpha, \quad (i = 1, 2, 3), \\ \vec{R} &= \vec{R}_\alpha - \vec{r}_5, \\ \vec{R}_{c.m.} &= \frac{1}{5}(4\vec{R}_\alpha + \vec{r}_5). \end{aligned} \quad (10)$$

Because of the particular structure of the wave function  $\Psi$ , the degree of freedom associated with the c.m. motion can be handled easily and, hence, will not be discussed.

After we sum over the spin and isospin coordinates and carry out the variational procedure, Eq. (6) is reduced to

$$\begin{aligned} \int \phi(1234)(\mathcal{K}_0 - E')\Psi(1234; 5)d\vec{r}_1 d\vec{r}_2 d\vec{r}_3 \\ = \int \phi(1234)(\mathcal{K}_1 - E')\Psi(5234; 1)d\vec{r}_1 d\vec{r}_2 d\vec{r}_3, \end{aligned} \quad (11)$$

where we have introduced the notation

$$\Psi(1234; 5) = \phi(1234)F(\vec{R}), \quad (12)$$

and

$$\begin{aligned} \Psi(5234; 1) &= P_{15}^r \Psi(1234; 5) \\ &= \int \phi(1234) \exp[-\frac{2}{5}\alpha(R^2 - R'^2)]F(\vec{R}') \\ &\quad \times \delta(\vec{R}' + \frac{1}{4}\vec{R} + \frac{5}{4}\vec{r}_1)d\vec{R}', \end{aligned} \quad (13)$$

with  $P^r$  being the space-exchange operator and  $\delta$  being the Dirac  $\delta$  function. Also, in Eq. (11), the quantities  $\mathcal{K}_0$  and  $\mathcal{K}_1$  are defined as

$$\begin{aligned} \mathcal{K}_0 &= T_\alpha - \frac{\hbar^2}{2\mu}\nabla_R^2 + \frac{e^2}{r_{24}} - V_0(6w + 6m)v_{12} \\ &\quad - V_0(4w - m + 2b - 2h)v_{15}, \end{aligned} \quad (14)$$

and

$$\begin{aligned} \mathcal{K}_1 &= T_\alpha - \frac{\hbar^2}{2\mu}\nabla_R^2 + \frac{e^2}{r_{24}} + V_0(-w + 4m - 2b + 2h)v_{15} \\ &\quad + V_0(-3w - 3m)(v_{12} + v_{25}) + V_0(-3w - 3m)v_{23}, \end{aligned} \quad (15)$$

with  $T_\alpha$  being the  $\alpha$ -particle kinetic energy operator and  $v_{ij}$  being the form factor of the nucleon-nucleon potential, given by

$$v_{ij} = e^{-\kappa r_{ij}^2}. \quad (16)$$

It should be noted that in Eq. (11), the left side gives rise to the usual direct terms, while the right side contains the nonlocal exchange terms.

Equation (11) can be further simplified by carrying out the integration on the left side and using the equation

$$E' = E_\alpha + E, \quad (17)$$

with

$$\begin{aligned} E_\alpha &= \int \phi(1234) \left[ T_\alpha - V_0(6w + 6m)v_{12} + \frac{e^2}{r_{24}} \right] \\ &\quad \times \phi(1234)d\vec{r}_1 d\vec{r}_2 d\vec{r}_3. \end{aligned} \quad (18)$$

The result is

$$\left[ \frac{\hbar^2}{2\mu}\nabla_R^2 + E - V_D(\vec{R}) \right] F(\vec{R}) = \mathcal{K}_1 + \mathcal{K}_2 + \mathcal{K}_3, \quad (19)$$

with

$$\begin{aligned} V_D &= -V_0(4w - m + 2b - 2h) \\ &\quad \times \int \phi(1234)v_{15}\phi(1234)d\vec{r}_1 d\vec{r}_2 d\vec{r}_3, \end{aligned} \quad (20)$$

$$\begin{aligned} \mathcal{K}_1 &= \int \phi(1234) [-V_0(-w + 4m - 2b + 2h)v_{15}] \\ &\quad \times \Psi(5234; 1)d\vec{r}_1 d\vec{r}_2 d\vec{r}_3, \end{aligned} \quad (21)$$

$$\begin{aligned} \mathcal{K}_2 &= \int \phi(1234) [-V_0(-3w - 3m)(v_{12} + v_{25})] \\ &\quad \times \Psi(5234; 1)d\vec{r}_1 d\vec{r}_2 d\vec{r}_3, \end{aligned} \quad (22)$$

and

$$\begin{aligned} \mathcal{K}_3 &= \int \phi(1234) \left[ \frac{\hbar^2}{2\mu}\nabla_R^2 - T_\alpha - \frac{e^2}{r_{24}} + E' \right. \\ &\quad \left. - V_0(-3w - 3m)v_{23} \right] \Psi(5234; 1)d\vec{r}_1 d\vec{r}_2 d\vec{r}_3. \end{aligned} \quad (23)$$

The quantity  $V_D$  is the familiar direct potential between the  $\alpha$  particle and the incident neutron; as is evident from Eq. (20), it is obtained by fold-

ing the direct part of the nucleon-nucleon potential into the  $\alpha$ -particle matter-density distribution. The quantities  $\mathcal{K}_1$ ,  $\mathcal{K}_2$ , and  $\mathcal{K}_3$  are nonlocal terms, arising from the use of a totally antisymmetric wave function in our calculations.

It is important to note that since Eq. (19) is obtained with antisymmetrization taken fully into account, we are allowed to consider the individual nucleons as distinguishable in our interpretation of the physical meaning of the quantities  $V_D$ ,  $\mathcal{K}_1$ ,  $\mathcal{K}_2$ , and  $\mathcal{K}_3$ . That is, in the original configuration before scattering, particle 1 is a neutron with spin up in the  $\alpha$  particle and particle 5 is the incident neutron also with spin up. Thus,  $V_D$  is a potential responsible for the direct process in which the incident neutron 5 interacts with the target nucleons and becomes scattered. The quantity  $\mathcal{K}_1$ , on the other hand, is responsible for the process in which the incident neutron 5 interacts

with the target neutron 1, with the consequence that 5 replaces 1 in the  $\alpha$  particle and neutron 1 is the scattered particle. This type of process is commonly called a knockout process. Similarly, the quantity  $\mathcal{K}_2$  describes a process involving an exchange of neutrons 1 and 5. But in this case, these neutrons interact not with each other as is the case for  $\mathcal{K}_1$ , but with other nucleons (nucleons 2, 3, 4) in the  $\alpha$  particle. This process involving  $\mathcal{K}_2$  is therefore a heavy-particle-pickup process. The term  $\mathcal{K}_3$  is somewhat harder to interpret physically. It arises from the fact that the correlation structure of the four-nucleon system (5234) is different from that of an  $\alpha$  particle. In this paper, we shall refer to  $\mathcal{K}_3$  as the nucleon-rearrangement term.

To complete the formulation, we explicitly carry out the integration over the internal coordinates in Eqs. (20)–(23). This yields

$$V_D = -V_0(4w - m + 2b - 2h) \left( \frac{4\alpha}{4\alpha + 3\kappa} \right)^{3/2} \exp\left( -\frac{4\alpha\kappa}{4\alpha + 3\kappa} R^2 \right), \quad (24)$$

and

$$\mathcal{K}_i = \int K_i(\vec{R}, \vec{R}') F(\vec{R}) d\vec{R}', \quad (25)$$

where

$$K_1(\vec{R}, \vec{R}') = -V_0 \left( \frac{4}{5} \right)^3 \left( \frac{4\alpha}{3\pi} \right)^{3/2} (-w + 4m - 2b + 2h) \exp\left[ -\frac{34\alpha + 48\kappa}{75} (R^2 + R'^2) - \frac{32\alpha - 96\kappa}{75} \vec{R} \cdot \vec{R}' \right], \quad (26)$$

$$K_2(\vec{R}, \vec{R}') = -V_0 \left( \frac{4}{5} \right)^3 \left( \frac{4\alpha}{3\pi} \right)^{3/2} (-3w - 3m) \left( \frac{3\alpha}{3\alpha + 2\kappa} \right)^{3/2} \\ \times \left[ \exp\left( -\frac{34\alpha^2 + 28\alpha\kappa}{75\alpha + 50\kappa} R^2 - \frac{34\alpha^2 + 108\alpha\kappa}{75\alpha + 50\kappa} R'^2 - \frac{32\alpha^2 + 64\alpha\kappa}{75\alpha + 50\kappa} \vec{R} \cdot \vec{R}' \right) \right. \\ \left. + \exp\left( -\frac{34\alpha^2 + 108\alpha\kappa}{75\alpha + 50\kappa} R^2 - \frac{34\alpha^2 + 28\alpha\kappa}{75\alpha + 50\kappa} R'^2 - \frac{32\alpha^2 + 64\alpha\kappa}{75\alpha + 50\kappa} \vec{R} \cdot \vec{R}' \right) \right], \quad (27)$$

and

$$K_3(\vec{R}, \vec{R}') = \left( \frac{4}{5} \right)^3 \left( \frac{4\alpha}{3\pi} \right)^{3/2} \left\{ -\frac{\hbar^2}{2M} \left[ \frac{47}{5} \alpha - \frac{1216}{1125} \alpha^2 (R^2 + R'^2) - \frac{1598}{1125} \alpha^2 \vec{R} \cdot \vec{R}' \right] - V_0 (-3w - 3m) \left( \frac{\alpha}{\alpha + 2\kappa} \right)^{3/2} + E' - e^2 \left( \frac{2\alpha}{\pi} \right)^{1/2} \right\} \\ \times \exp\left[ -\frac{34}{75} \alpha (R^2 + R'^2) - \frac{32}{75} \alpha \vec{R} \cdot \vec{R}' \right]. \quad (28)$$

In the following discussion, we shall refer to  $K_1$ ,  $K_2$ , and  $K_3$  as the knockout, heavy-particle-pickup, and nucleon-rearrangement kernels, respectively. Using Eqs. (24)–(28), we can then solve Eq. (19) by the usual method of partial waves to obtain the phase shifts and subsequently elastic scattering differential cross sections.

To have confidence about the conclusion to be reached in this investigation concerning the fea-

tures of the antisymmetrization effects, we should make certain, of course, that our calculation does yield results in reasonable agreement with experiment. For this purpose we have calculated the  $p + \alpha$  differential cross section at  $E = 76$  MeV and made a comparison with the experimental data of Selove and Teem.<sup>9</sup> This is shown in Fig. 1, where one sees that even at this rather high energy there is fair agreement, indicating that the

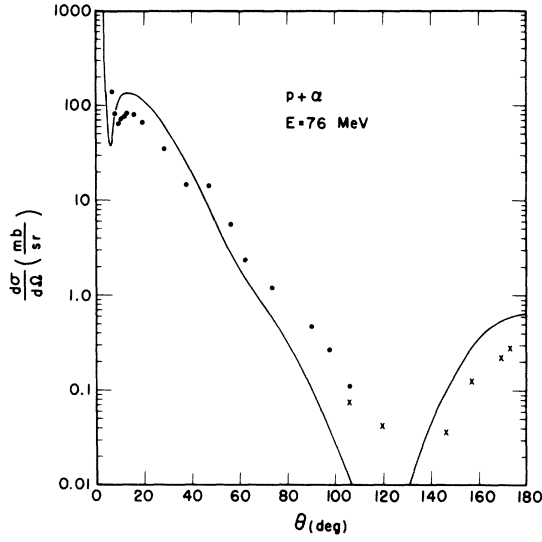


FIG. 1. Comparison of the calculated differential cross section for  $p+\alpha$  scattering with experimental data at 76 MeV. The experimental data are those of Ref. 9.

main features of this five-nucleon scattering problem are indeed included in our simplified formulation.

### III. BORN-APPROXIMATION RESULTS

As a first step in our attempt to understand the roles played by the direct potential  $V_D$  and the kernels  $K_1$ ,  $K_2$ , and  $K_3$ , we study the behavior of the scattering amplitudes in the Born approximation

$$f_1 = \frac{\mu}{2\pi\hbar^2} V_0(-w+4m-2b+2h) \left(\frac{16\pi}{3\alpha+16\kappa}\right)^{3/2} \exp\left[-\frac{25}{4(3\alpha+16\kappa)}k^2\right] \exp\left[-\frac{4(3\kappa-\alpha)}{\alpha(3\alpha+16\kappa)}k^2 \sin^2\left(\frac{\theta}{2}\right)\right], \quad (32)$$

$$f_2 = -2\frac{\mu}{2\pi\hbar^2} V_0(3w+3m) \left(\frac{16\pi}{3\alpha+10\kappa}\right)^{3/2} \exp\left[-\frac{9(\alpha+2\kappa)}{4\alpha(3\alpha+10\kappa)}k^2\right] \exp\left[-\frac{4(\alpha+2\kappa)}{\alpha(3\alpha+10\kappa)}k^2 \cos^2\left(\frac{\theta}{2}\right)\right], \quad (33)$$

$$f_3 = -\frac{\mu}{2\pi\hbar^2} \left(\frac{16\pi}{3\alpha}\right)^{3/2} \left\{ E_\alpha - V_0(-3w-3m) \left(\frac{\alpha}{\alpha+2\kappa}\right)^{3/2} - e^2 \left(\frac{2\alpha}{\pi}\right)^{1/2} - \frac{\hbar^2}{2M} \left[ 3\alpha + \frac{3}{4}k^2 + \frac{4}{3}k^2 \cos^2\left(\frac{\theta}{2}\right) \right] \right\} \times \exp\left(-\frac{3}{4\alpha}k^2\right) \exp\left[-\frac{4}{3\alpha}k^2 \cos^2\left(\frac{\theta}{2}\right)\right]. \quad (34)$$

The differential scattering cross section is, of course, simply given by

$$\frac{d\sigma}{d\Omega} = |f_D + f_1 + f_2 + f_3|^2. \quad (35)$$

The validity of the Born approximation in the energy region of interest can be tested by making a comparison between the differential cross section calculated by a numerical solution of the integrodifferential equation (19) using the method of

corresponding to these terms. This will be carried out in the energy region above 50 MeV, since as will be demonstrated below, the Born approximation is reasonably valid for the  $n+\alpha$  problem at these relatively high energies.

The Born scattering amplitude for the direct potential  $V_D$  is given by

$$f_D = -\frac{\mu}{2\pi\hbar^2} \int e^{-i\vec{k}_f \cdot \vec{R}} V_D(R) e^{i\vec{k}_i \cdot \vec{R}} d\vec{R}, \quad (29)$$

with  $\vec{k}_i$  and  $\vec{k}_f$  being the initial and final propagation vectors. By using the explicit form of  $V_D$  given in Eq. (24) and performing the integration, one obtains

$$f_D = \frac{\mu}{2\pi\hbar^2} V_0(4w-m+2b-2h) \left(\frac{\pi}{\kappa}\right)^{3/2} \times \exp\left[-\frac{4\alpha+3\kappa}{4\alpha\kappa}k^2 \sin^2\left(\frac{\theta}{2}\right)\right], \quad (30)$$

where  $k = |\vec{k}_i| = |\vec{k}_f|$ , and  $\theta$  is the scattering angle in the c.m. system. Similarly, the scattering amplitudes for the kernel terms can be calculated with the equation

$$f_i = -\frac{\mu}{2\pi\hbar^2} \int e^{-i\vec{k}_f \cdot \vec{R}} K_i(\vec{R}, \vec{R}') e^{i\vec{k}_i \cdot \vec{R}'} d\vec{R} d\vec{R}'. \quad (31)$$

Using the expressions for  $K_i$  ( $i=1, 2, 3$ ) given in Eqs. (26)–(28), one can carry out the integration and obtain the following results:

the partial waves (hereafter referred to as the resonating-group or r-g calculation) and the differential cross section calculated in the Born approximation. Such a comparison at  $E=50$  MeV is shown in Fig. 2, where the resonating-group calculation and the Born-approximation results are represented by solid and dashed lines, respectively. From this figure it can be seen that even though there is some discrepancy, the Born result does reproduce the necessary features, i.e., the

occurrence of the diffraction minimum at around  $110^\circ$  and large cross sections at backward angles. Thus, we feel that a study of the behavior of the Born scattering amplitudes should give us a qualitative understanding of the roles played by the direct and exchange terms.

The Born amplitudes  $f_D$ ,  $f_1$ ,  $f_2$ , and  $f_3$  are plotted as a function of  $\theta$  at c.m. energies of 50 and 100 MeV in Fig. 3. Here it is seen that the direct amplitude  $f_D$  has a large magnitude at  $\theta=0^\circ$ , but decreases rapidly with angle. The amplitude  $f_1$  (knockout amplitude) is also peaked in the forward direction; it has a rather small magnitude, but decreases slowly as the angle increases. On the other hand, the amplitudes  $f_2$  (heavy-particle pickup amplitude) and  $f_3$  (nucleon-rearrangement amplitude) are important mainly at backward angles. They are, of course, chiefly responsible for the occurrence of large scattering cross sections at these angles. It should be emphasized again that the amplitudes  $f_2$  and  $f_3$  arise as a consequence of the antisymmetrization procedure. This indicates, therefore, that the differential cross section in the backward angular region is closely related to the exchange effects. If these effects are not properly accounted for, then it is our opinion that a satisfactory description of the experimental phenomena at large scattering angles will be a very difficult task.<sup>10</sup>

From Fig. 3 it can be further seen that at least in the  $n + \alpha$  case, the knockout amplitude  $f_1$  seems to play a relatively minor role. In fact, it makes a significant contribution only in the angular re-

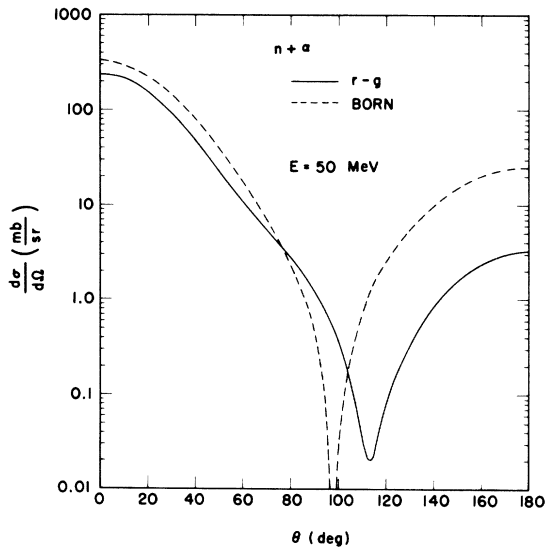


FIG. 2. Comparison of the differential cross section calculated by a numerical solution of the integrodifferential equation (19) (solid line) with the differential cross section calculated in the Born approximation (dashed line).

gion around  $90^\circ$ , where it interferes effectively with the other three amplitudes.

Based on the discussion given in Sec. II on the direct potential  $V_D$ , the knockout term  $\mathcal{K}_1$ , and the heavy-particle-pickup term  $\mathcal{K}_2$ , and using the features of the Born scattering amplitudes  $f_D$ ,  $f_1$ , and  $f_2$  learned here, we show in Fig. 4 a schematic representation of the  $n + \alpha$  problem as a sum of direct and exchange processes. Essentially, the purpose here is to demonstrate in a graphical way the mathematical contents of Eqs. (20)–(22) concerning  $V_D$ ,  $\mathcal{K}_1$ , and  $\mathcal{K}_2$ ; and Eqs. (30), (32), and (33) concerning the scattering amplitudes. It must be emphasized that such schematic representation should not be taken too literally, but rather should be considered only as a visual aid in appreciating the salient features of these processes. The nucleon-rearrangement process is not shown in this figure, since we know of no schematic way to demonstrate this particular process.

Next, we will construct equivalent local poten-

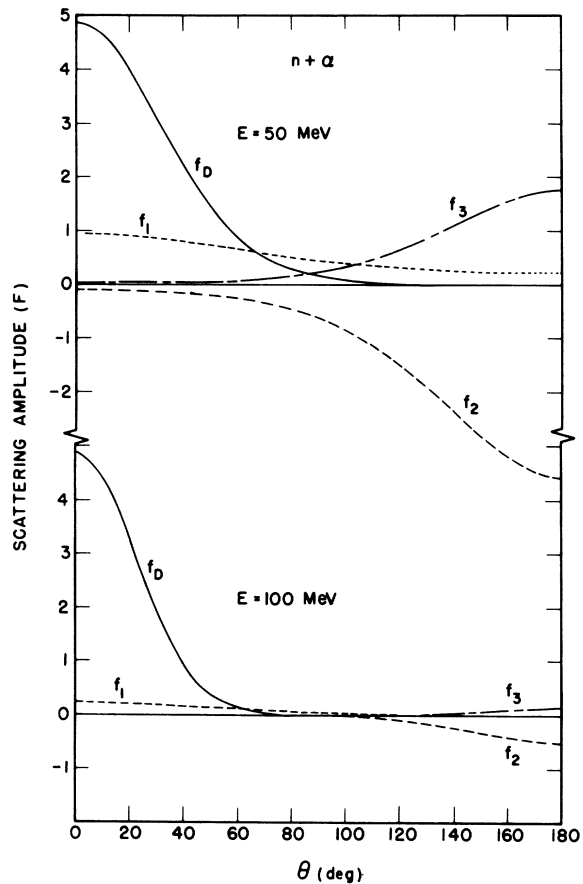


FIG. 3. Born scattering amplitudes for the direct process  $f_D$ , the knockout process  $f_1$ , the heavy-particle-pickup process  $f_2$ , and the nucleon-rearrangement process  $f_3$  at 50 and 100 MeV.

tials between the neutron and the  $\alpha$  particle which will yield the same scattering amplitudes in the Born approximation ( $f_1, f_2, f_3$ ) as the kernel terms  $K_1, K_2$ , and  $K_3$ . Recognizing the fact that for smoothly varying potentials at relatively high energies, the Born scattering amplitude for a

Wigner-type potential is large mainly in the forward directions, while the Born scattering amplitude for a Majorana-type potential is large mainly in the backward directions, we can easily find these equivalent potentials; these will be labeled as  $U_1, U_2$ , and  $U_3$ , and are given by

$$U_1 = V_1 = -V_0(-w + 4m - 2b + 2h) \left( \frac{4\alpha}{3\kappa - \alpha} \right)^{3/2} \exp \left[ -\frac{25}{4(3\alpha + 16\kappa)} k^2 \right] \exp \left[ -\frac{\alpha(3\alpha + 16\kappa)}{4(3\kappa - \alpha)} R^2 \right], \quad (36)$$

$$U_2 = V_2 P^R = 2V_0(3w + 3m) \left( \frac{4\alpha}{\alpha + 2\kappa} \right)^{3/2} \exp \left[ -\frac{9(\alpha + 2\kappa)}{4\alpha(3\alpha + 10\kappa)} k^2 \right] \exp \left[ -\frac{\alpha(3\alpha + 10\kappa)}{4(\alpha + 2\kappa)} R^2 \right] P^R, \quad (37)$$

$$U_3 = V_3 P^R = 8 \left[ E_\alpha - V_0(-3w - 3m) \left( \frac{\alpha}{\alpha + 2\kappa} \right)^{3/2} - e^2 \left( \frac{2\alpha}{\pi} \right)^{1/2} - \frac{\hbar^2}{2M} \left( \frac{3}{2}\alpha + \frac{3}{4}k^2 - \frac{3}{4}\alpha^2 R^2 \right) \right] \times \exp \left( -\frac{3}{4\alpha} k^2 \right) \exp \left( -\frac{3\alpha}{4} R^2 \right) P^R, \quad (38)$$

where  $P^R$  is a Majorana operator exchanging the position coordinates of the neutron and the  $\alpha$  particle. The total equivalent local interaction is, therefore,

$$V_T = (V_D + V_1) + (V_2 + V_3) P^R, \quad (39)$$

where  $V_1, V_2$ , and  $V_3$  are defined in Eqs. (36)–(38).

There are two important features in the equivalent local potentials which should be pointed out. First, the potentials  $V_1, V_2$ , and  $V_3$  are all explicitly energy dependent, while the direct potential  $V_D$  is not. Second, the total potential  $V_T$  contains a significant amount of Majorana component, which means that it takes on different values depending upon whether the relative orbital angular momentum between the neutron and the  $\alpha$  particle is even or odd.<sup>11</sup> It should be mentioned that this odd-even feature was found to be necessary in a phenomenological local-potential analysis of the  $p + \alpha$  scattering data by Gammel and Thaler.<sup>12</sup> More recently, the presence of such a feature in the equivalent local potential was further substantiated by a detailed study of the resonating-group wave functions.<sup>13</sup> Thus, it is indeed quite interesting that we can demonstrate the existence of this feature so clearly with our present rather simple considerations.

In Fig. 5, we show the behavior of the potential  $V_T$  in both even- and odd- $L$  states at an energy of 100 MeV. From this figure, one can easily see that the potentials in both  $L$  states are rather different from the direct potential  $V_D$  for small values of  $R$  ( $R \lesssim 1.5 F$ ) and the odd-even feature is quite evident even at this high energy.

To have some idea about the relative importance of the potentials  $V_D, U_1, U_2$ , and  $U_3$ , we calculate the volume integrals defined as

$$I_D = \int V_D d\vec{R}, \quad (40)$$

for the direct potential and

$$I_i = \int V_i d\vec{R} \quad (41)$$

for the exchange potentials. The values of these integrals are listed in Table I at energies from 50 to 150 MeV. From this table, we note that  $I_1/I_D$  is about 0.2 at 50 MeV and decreases to about 0.01 at 150 MeV. This indicates that for the Wigner part of the potential  $V_T$  given by Eq. (39), the direct potential  $V_D$  is the dominant term. As for the Majorana part of  $V_T$ , we see from Table I that even though  $I_3$  has a smaller magnitude than  $I_2$  at all energies, it is certainly not negligible. This means that the potential  $U_3$  plays a relatively minor role, but should still be included if an accurate description of the  $n + \alpha$  scattering problem is desired.

In Table I, we have also listed the values of  $R_{MW}$ , defined as

$$R_{MW} = (I_2 + I_3)/(I_D + I_1). \quad (42)$$

Here one sees that the value of  $R_{MW}$  at 50 MeV is equal to  $-0.309$ , which compares favorably with the value of  $-0.2 \pm 0.05$  obtained by Giamati *et al.* from a phenomenological study of the  $p + \alpha$  scattering data at 32 MeV.<sup>14</sup> The difference in magnitude is probably not a serious discrepancy, considering that our values are obtained from a Born-approximation calculation. Further, we note from this table that the magnitude of  $R_{MW}$  decreases rapidly with energy, being equal to only 0.011 at 150 MeV. We should emphasize, however, that this does not at all mean that we can omit the Majorana component in the total potential  $V_T$  at

these energies, since as has been mentioned before, the Wigner and Majorana components have their major contribution in different angular regions.

#### IV. FURTHER STUDY OF KERNEL FUNCTIONS

In this section, we further study the effects of the knockout, heavy-particle-pickup, and nucleon-

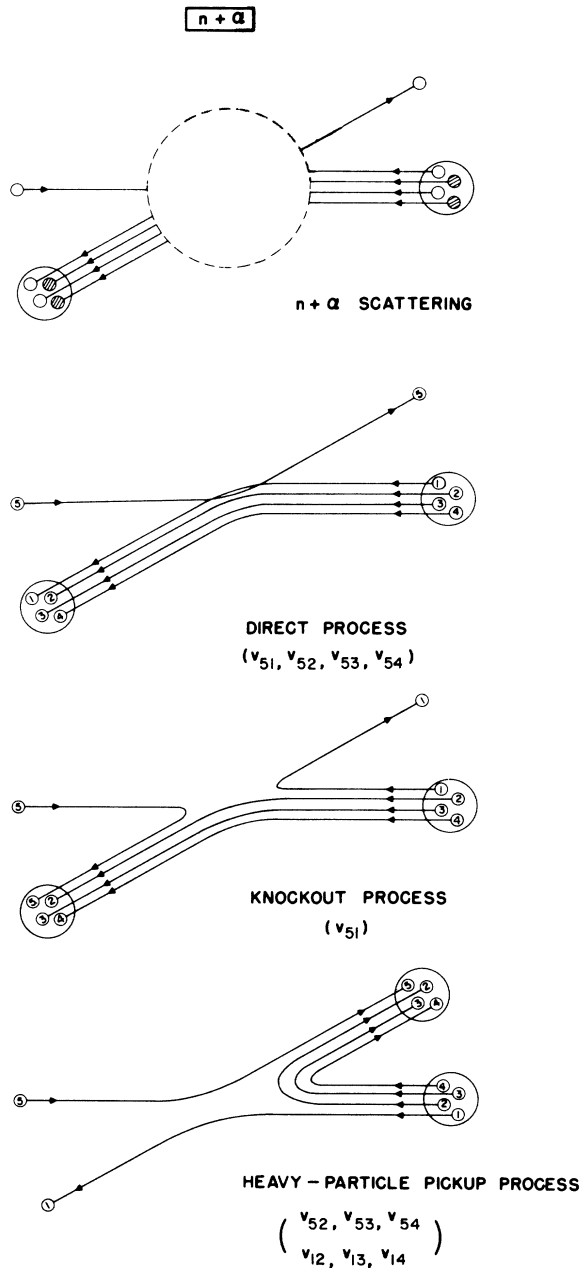


FIG. 4. Schematic representation of the  $n + \alpha$  scattering problem as a sum of direct and exchange processes. The nucleon-rearrangement process is not shown.

rearrangement kernels by solving the integrodifferential equation (19) numerically with various combinations of these kernels set as zero. The purpose is to ascertain the validity of the conclusions reached in Sec. III with the Born approximation. What we shall do is to compare the differential cross section calculated with all the kernel functions included (to be referred to as the full resonating-group calculation) and the differential cross sections calculated with one or more of the kernel functions left out. It is necessary to perform this study in this indirect manner, since it is only in the Born approximation that one can separate the total scattering amplitude into a sum of direct, knockout, heavy-particle-pickup, and nucleon-rearrangement amplitudes.

In Fig. 6, the solid lines show the differential cross sections at 50 and 100 MeV obtained with the full resonating-group calculation. The crosses represent the result obtained using the direct potential  $V_D$  only; the kernel functions  $K_1$ ,  $K_2$ , and  $K_3$  of Eqs. (26)–(28) are set equal to zero, thus disregarding antisymmetrization effects completely. From this figure it can be seen that the most prominent feature of this comparison is obviously the lack of a rise in the differential cross section at backward angles for the case where only  $V_D$  is included. This therefore supports our

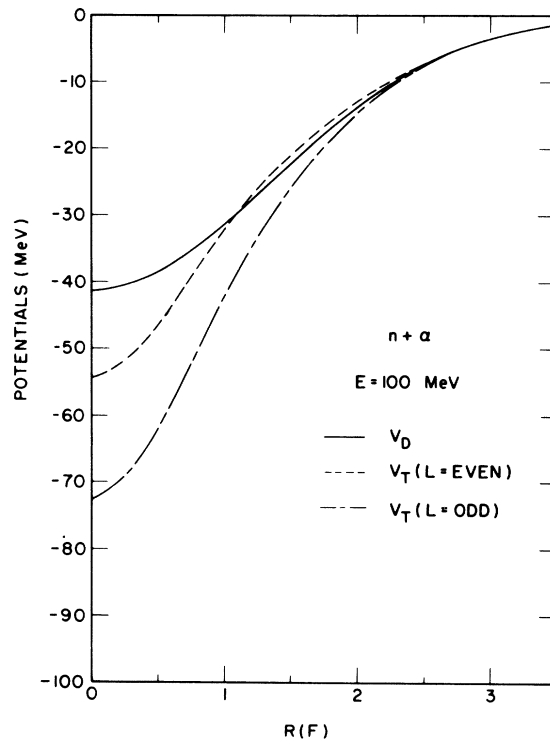


FIG. 5. Equivalent  $n + \alpha$  local potential at 100 MeV in even- and odd-orbital-angular-momentum states.

TABLE I. Volume integrals and Majorana-to-Wigner ratio of the equivalent local potentials in the  $n + \alpha$  system.

$E$ (MeV)	$I_D$ (MeV F <sup>3</sup> )	$I_1$ (MeV F <sup>3</sup> )	$I_2$ (MeV F <sup>3</sup> )	$I_3$ (MeV F <sup>3</sup> )	$R_{MW}$
50	-1592.6	-309.1	1163.6	-574.3	-0.309
75	-1592.6	-157.0	434.2	-181.4	-0.144
100	-1592.6	-79.8	161.9	-54.4	-0.065
120	-1592.6	-46.3	73.6	-20.2	-0.032
150	-1592.6	-20.5	22.5	-4.6	-0.011

finding in the Born approximation that, at the energies under consideration, the exchange effects are very important in the backward angular region, where the direct potential  $V_D$  makes, in fact, only an insignificant contribution.

Figure 7 compares the full resonating-group calculation with a calculation in which the knock-out kernel  $K_1$  of Eq. (26) is set to be equal to zero. Here one sees that the absence of the  $K_1$  term is

noticeable mainly in the intermediate angular region. This is again consistent with our finding that the Born amplitude  $f_1$  is rather small and should manifest itself only in this angular region through interference with the other Born amplitudes. Also, as is found in Sec. III, the omission of  $K_1$  has a slightly larger effect at 50 MeV than at 100 MeV.

Finally, in Fig. 8, we show the result of a calculation in which the heavy-particle-pickup kernel  $K_2$  and the nucleon-rearrangement kernel  $K_3$  are set as equal to zero. From this figure we can easily conclude that the large backward-angle cross sections are produced by the  $K_2$  and  $K_3$  terms, again in agreement with the Born-approximation result. As for the forward angular region, one sees here that the influence of these two terms is almost not noticeable, indicating that they have very little contribution in this particular region.

In summary, this study shows that, at the energies considered here, the conclusions reached by the simple Born-approximation consideration,

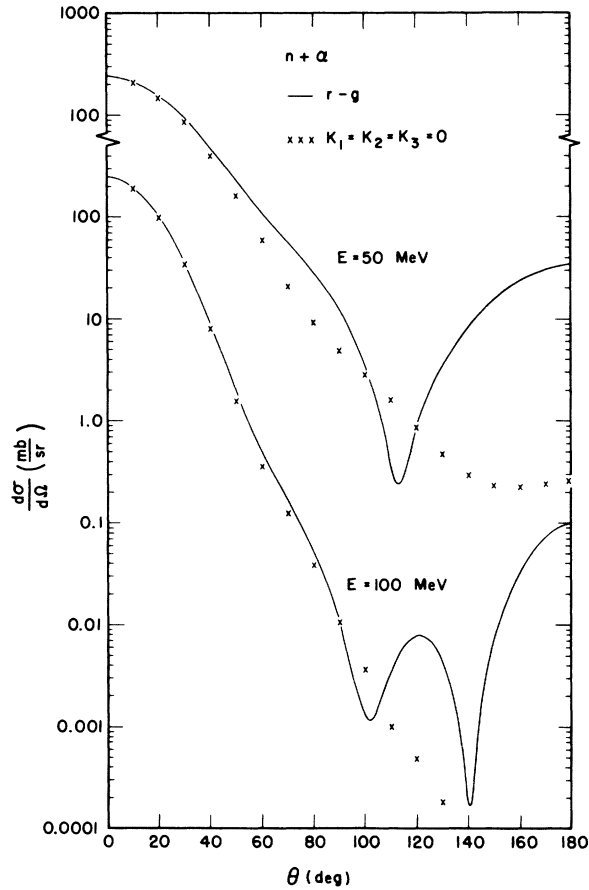


FIG. 6. Comparison of the differential cross sections obtained with the full resonating-group calculation and the differential cross sections obtained using the direct potential  $V_D$  only.

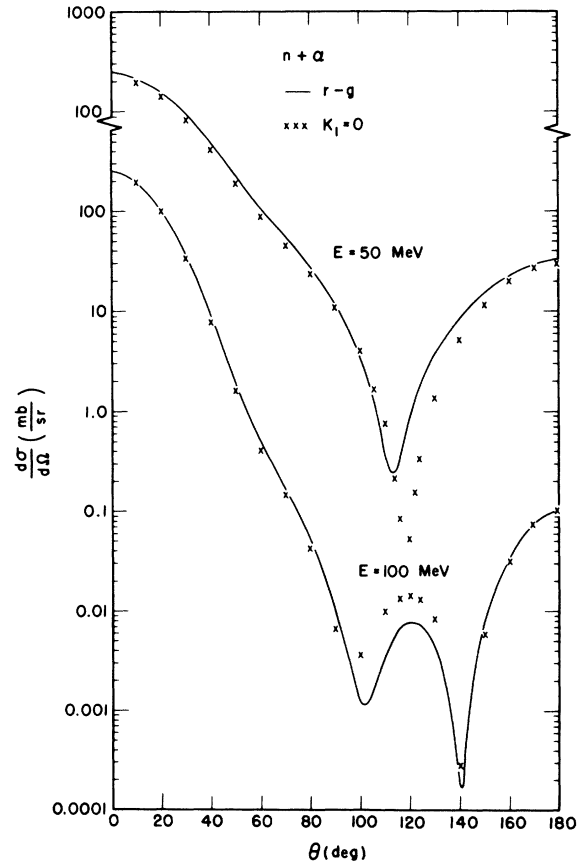


FIG. 7. Comparison of the differential cross section obtained with the full resonating-group calculation and the differential cross sections obtained with  $K_1$  set to zero.

as described in Sec. III, are quite valid. Therefore, the features of the scattering amplitudes and equivalent potentials learned there can be used as a guide to devise approximation methods in handling those systems where a full resonating-group calculation is impractical. This will be discussed in the next section.

#### V. APPROXIMATION METHODS FOR HEAVIER SYSTEMS

Having established that the Born-approximation results are fairly reliable, we now proceed to use these results to find ways of approximating a full resonating-group calculation. From Fig. 3, we note that the Born amplitudes  $f_2$  and  $f_3$  are nearly proportional to each other in the angular region where they have significant magnitudes. This suggests that if we replace  $\mathcal{K}_3$  in Eq. (19) by  $\gamma\mathcal{K}_2$ , with  $\gamma$  being an energy-dependent constant, and solve instead the integrodifferential equation

$$\left[ \frac{\hbar^2}{2\mu} \nabla_R^2 + E - V_D(\vec{R}) \right] F(\vec{R}) = \mathcal{K}_1 + C\mathcal{K}_2 \quad (43)$$

with  $C = 1 + \gamma$ , we may obtain results similar to those of the full resonating-group calculation. To see if this is indeed so, we have solved Eq. (43) numerically at 20, 50, and 100 MeV, and adjusted  $C$  to yield the best agreement with the full calculation at these energies. The result is shown in Fig. 9, where the solid curves show the differential cross sections obtained with the full resonating-group calculation, while the crosses represent the differential cross sections obtained using Eq. (43) with appropriate values of  $C$ . From this figure it is evident that there exists a value of  $C$  at each energy which enables us to use Eq. (43) to approximate the full resonating-group calculation quite closely. In fact, it can be seen that our approximation is good even at 20 MeV; this is interesting, since Eq. (43) is based on the results of

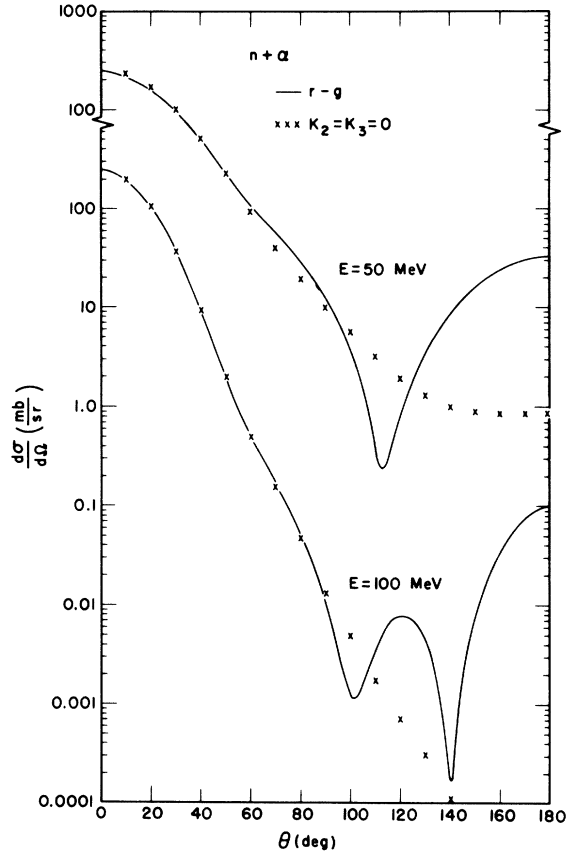


FIG. 8. Comparison of the differential cross sections obtained with the full resonating-group calculation and the differential cross sections obtained with  $K_2$  and  $K_3$  set to zero.

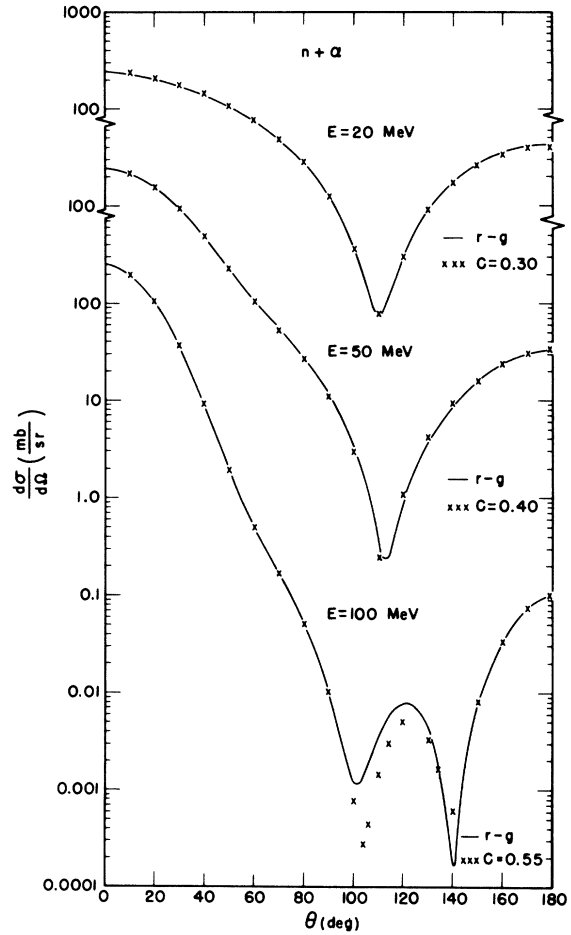


FIG. 9. Comparison of the differential cross sections obtained with the full resonating-group calculation and the differential cross sections obtained using Eq. (43) with appropriate values of  $C$ .

the Born-approximation study, which is not expected to be too reliable at such a low energy.

The values of  $C$  are equal to 0.3, 0.4, and 0.55 at energies of 20, 50, and 100 MeV, respectively. The fact that it increases with energy is just a reflection of the Born-approximation finding that the ratio of the magnitudes of  $I_3$  to  $I_2$  (see Table I) becomes smaller as the energy increases.

In the  $n + \alpha$  system itself, it is of course not necessary to employ this approximate procedure, since here the derivation of the kernels  $K_1$ ,  $K_2$ , and  $K_3$  is quite simple. On the other hand, if one wishes to consider such problems as the scattering of nucleons by medium- and heavy-weight nuclei, then one will soon find that while the derivation of the terms  $V_D$ ,  $K_1$ , and  $K_2$  is relatively straightforward; the derivation of the kernel  $K_3$  may be quite difficult. Thus, in these cases, it will be advantageous to use Eq. (43) and adjust  $C$  at each energy to get the best agreement with experiment. It is realized, of course, that the adjustment of  $C$  is entirely a phenomenological procedure, but we feel that this is a minor disadvantage, considering the fact that the essential features of antisymmetrization are still contained in this approximation method.

At present, we are making a very preliminary test on this approximation method by considering the  $p + \text{Ca}^{40}$  scattering problem at about 30 MeV. What we do is to omit  $K_1$ ,<sup>15</sup> replace  $V_D$  in Eq. (43) by the usual local optical potential complete with imaginary and spin-orbit parts, and characterize  $K_2$  by a simple form similar in nature to the kernel  $K_2$  of Eq. (27). The result shows that the experimental data, in particular the polarization data, can indeed be much better represented if  $C$  is chosen to be not equal to zero.<sup>16</sup> Similar consideration of the  $p + \text{Ni}^{58}$  scattering problem has yielded a similar conclusion.

The Born-approximation study further shows that an equivalent local potential between clusters should contain a Majorana component. This suggests that a better description of the  $p + \text{nucleus}$  scattering data may be obtained if the real central part of the optical potential is modified to contain this particular feature. At this moment, we are also making a calculation on  $p + \text{Ca}^{40}$  scattering to determine whether this is the case, and preliminary results are indeed very encouraging.

## VI. CONCLUSION

The  $n + \alpha$  scattering problem is studied with the method of the resonating-group structure, the purpose being to understand the effects of the requirement that the wave function for this system be antisymmetric with respect to the exchange of the incident neutron with the neutrons in the  $\alpha$  particle. With a one-channel approximation the resultant integrodifferential equation describing the relative motion between these two particles is found to contain a direct-potential term, obtained by folding the direct part of the nucleon-nucleon potential into the matter-density distribution of the  $\alpha$  particle, and a kernel function, arising explicitly from the antisymmetrization procedure. The kernel function is shown to be separable into three terms, corresponding to knockout, heavy-particle-pickup, and nucleon-rearrangement processes.

At the energies under consideration (50 to 100 MeV), the direct potential and the knockout kernel are shown to contribute mainly in the forward directions, while the heavy-particle-pickup kernel and the nucleon-rearrangement kernel are shown to contribute mainly in the backward directions. In particular, it is found that these two latter kernels are almost entirely responsible for the occurrence of large backward-angle cross sections in the  $n + \alpha$  problem, thus fully demonstrating the importance of the antisymmetrization procedure, at least in the lighter nuclear systems.

In the Born approximation, it is further shown that an equivalent local potential can be constructed between the neutron and the  $\alpha$  particle, which yields the same results as does the resonating-group calculation. This equivalent local potential has the notable features of being explicitly energy dependent and having a significant amount of Majorana space-exchange component.

With the knowledge learned here, we have also proposed approximation methods which contain the essential features of antisymmetrization and yet could be used to consider such more complicated problems as the scattering of nucleons by medium- and heavy-weight nuclei. At present, we are using these methods to study  $p + \text{Ca}^{40}$  scattering, and preliminary calculations do yield results which are very encouraging.

\*Work supported in part by the U. S. Atomic Energy Commission under Contract Nos. AT(11-1)-1764 and AT(11-1)-1265.

†A preliminary account of this work was presented at the American Physical Society, New York meeting, 1971

[Bull. Am. Phys. Soc. 16, 77 (1971)].

<sup>1</sup>Y. C. Tang, in *Proceedings of the International Conference on Clustering Phenomena in Nuclei, Bochum, Germany, 1969* (International Atomic Energy Agency, Vienna, Austria, 1969), p. 109, and references con-

tained therein.

<sup>2</sup>I. Reichstein and Y. C. Tang, Nucl. Phys. **A139**, 144 (1969); **A158**, 529 (1970).

<sup>3</sup>J. A. Wheeler, Phys. Rev. **52**, 1083 (1937).

<sup>4</sup>K. Wildermuth and W. McClure, *Cluster Representations of Nuclei* (Springer-Verlag, Berlin, 1966).

<sup>5</sup>See, for example, G. W. Greenlees, G. J. Pyle, and Y. C. Tang, Phys. Rev. **171**, 1115 (1968).

<sup>6</sup>D. R. Thompson, I. Reichstein, W. McClure, and Y. C. Tang, Phys. Rev. **185**, 1351 (1969).

<sup>7</sup>A similar treatment has been reported by A. Herzenberg and E. J. Squires [Nucl. Phys. **19**, 280 (1960)]. We should mention, however, that in their paper there is a factor of 2 missing in the Born scattering amplitude for the heavy-particle-pickup process. Also, these authors have not considered the nucleon-rearrangement process which arises as a consequence of the antisymmetrization procedure.

<sup>8</sup>I. Reichstein, D. R. Thompson, and Y. C. Tang, Phys. Rev. C **3**, 2139 (1971).

<sup>9</sup>W. Selove and J. M. Teem, Phys. Rev. **112**, 1658 (1958).

<sup>10</sup>R. E. Brown, E. E. Gross, and A. van der Woude, Phys. Rev. Letters **25**, 1346 (1970); W. Fetscher, K. Sattler, N. C. Schmeing, E. Seibt, C. Weddigen, and E. J. Kanellopoulos, Phys. Letters **34B**, 171 (1971).

<sup>11</sup>It is interesting to note that the equivalent Coulomb exchange potential, contained in  $U_3$ , is a Majorana-type potential.

<sup>12</sup>J. L. Gammel and R. M. Thaler, Phys. Rev. **109**, 2041 (1958).

<sup>13</sup>R. E. Brown and Y. C. Tang, Phys. Rev. **176**, 1235 (1968).

<sup>14</sup>C. C. Giamati, V. A. Madsen, and R. M. Thaler, Phys. Rev. Letters **11**, 163 (1963).

<sup>15</sup>In a later and more detailed investigation, we shall also include a kernel of the  $K_1$  type in the analysis. In the present preliminary study, we have omitted this type of kernel mainly for simplicity, but also from the observation that, in the  $n + \alpha$  case, the effect of  $K_1$  is relatively unimportant.

<sup>16</sup>G. W. Greenlees, Y. C. Tang, and D. R. Thompson, to be published.

## Polarization Measurements of the Gamma-Ray Transitions from the 1.459-MeV Level in $^{19}\text{F}$

K. A. Hardy, A. H. Lumpkin, Y. K. Lee, and G. E. Owen

*Department of Physics, The Johns Hopkins University, Baltimore, Maryland 21218*

(Received 5 April 1971)

Linear-polarization and angular-distribution measurements have been made on the three transitions from the 1.459-MeV level in  $^{19}\text{F}$  using inelastic proton scattering. The mixing ratios were determined to be  $-0.1 < \delta_{M2/E1} < 0.0$  for the 1.459  $\rightarrow$  0.197-MeV transition,  $0.30 < \delta_{E2/M1} < 0.38$  for the 1.459  $\rightarrow$  0.110-MeV transition, and  $|\delta_{M2/E1}| < 0.06$  for the 1.459  $\rightarrow$  0-MeV transition. The results indicate that the level in question cannot be explained as a  $p_{1/2}$  proton hole coupled to the pure ground-state rotational band as has been accepted in the past.

### I. INTRODUCTION

The nucleus  $^{19}\text{F}$  has been the subject of several recent theoretical<sup>1-4</sup> and experimental<sup>5-8</sup> investigations, and the detailed properties of the low-lying states of this nucleus are now fairly well understood. In particular, Benson and Flowers<sup>1</sup> successfully explained the low-lying positive-parity levels in  $^{19}\text{F}$  by shell-model calculations as three nucleons coupled to an  $^{16}\text{O}$  core, and the authors attempted further to explain the negative-parity levels as a  $p_{1/2}$  proton hole coupled to the ground-state rotational band in  $^{20}\text{Ne}$ .

The crucial test for this "one-band" model for the  $\frac{3}{2}^-$  and  $\frac{5}{2}^-$  states in  $^{19}\text{F}$  comes from the observation that the  $E2$  strength for the transitions 1.459  $\rightarrow$  0.110 and 1.346  $\rightarrow$  0.110 MeV in  $^{19}\text{F}$  should be the same as the 1.630  $\rightarrow$  0-MeV transition in  $^{20}\text{Ne}$  if the odd-parity states in  $^{19}\text{F}$  indeed arise

from the coupling of a proton hole to the ground-state rotational band of  $^{20}\text{Ne}$ . The  $E2$  strength of the transitions can be obtained by measurement of the mixing ratio and the lifetime of the states.

The mixing ratio in question can be determined by a linear polarization measurement of the  $\gamma$  ray. Such a measurement is difficult, however, because of the background from three other  $\gamma$  rays of nearly equal energy. As soon as a polarimeter based on germanium detectors became available, Lam, Litherland, and Simpson<sup>8</sup> were able to resolve the  $\gamma$  rays and measure the mixing ratios, but their single-crystal polarimeter did not have a large enough asymmetry ratio to prove or disprove the prediction of Benson and Flowers. Recently in our laboratory, a polarimeter constructed with two planar germanium detectors has been built. This polarimeter has an improved asymmetry ratio which is suitable for an experi-